Y. Li, P. Badrinarayana, M. R. Kessler: Liquid Crystalline Epoxy Resin Based on Biphenyl Mesogen: Thermal Characterization, *Polymer*, 2013, 54(12), 3017-3025. doi:10.1016/j.polymer.2013.03.043

Liquid crystalline epoxy resin based on biphenyl mesogen: Thermal characterization

Yuzhan Li[a], Prashanth Badrinarayanan[b], Michael R. Kessler[a, c,]

[a] Department of Materials Science and Engineering, Iowa State University, Ames, IA 50011, USA

[b] DuPont, 200 Powder Mill Road, Wilmington, DE 19803, USA

[c] Ames Laboratory, US Department of Energy, Ames, IA 50011, USA

Abstract

An epoxy monomer of 4,4′-diglycidyloxybiphenyl (BP) was synthesized and cured with a tetra-functional amine, sulfanilamide (SAA), to produce novel liquid crystalline epoxy resins (LCERs). The thermal properties, liquid crystalline morphologies, and cure behavior of the monomer were studied using differential scanning calorimetry, wide angle X-ray diffraction, and polarized optical microscopy. The effects of curing condition on the glass transition temperature, coefficient of thermal expansion, and dynamic mechanical properties of the resins were determined through thermomechanical analysis and dynamic mechanical analysis, respectively. The effects of cure condition on the formation of the liquid crystalline phase were also examined. The results show that BP is not a liquid crystalline epoxy monomer and an irreversible crystal transition exists in the temperature range of 120 °C–140 °C. The use of SAA results in the formation of a smectic liquid crystalline phase. Compared to the resins cured into an amorphous network, the LCERs exhibited a polydomain structure with individual liquid crystalline domain distributed in the resin matrix, which results in better thermomechanical properties.

Graphical abstract

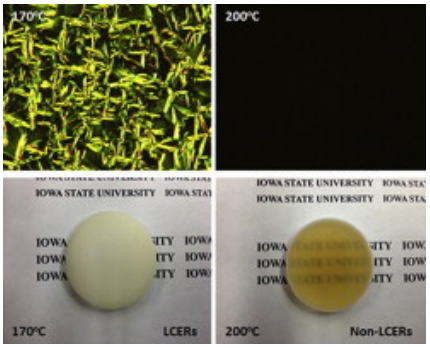

Keywords

- Liquid crystalline epoxy resins (LCERs);
- Curing;
- Thermomechanical properties

1. Introduction

Liquid crystalline thermosets (LCTs) are a unique class of thermosetting materials formed upon curing of low molecular weight, rigid rod, multifunctional monomers resulting in the retention of a liquid crystalline phase by the three dimensional crosslinking networks. A great number of LCTs based on different functional end groups have been synthesized and studied [1], [2] and [3], including epoxy [4], [5], [6], [7], [8] and [9], acrylate [10], [11] and [12], maleimide [13] and [14], and cyanate ester [15] and [16]. Liquid crystalline epoxy resins (LCERs) are of great interest to scientists and engineers and have been investigated because of their unique properties, e.g. low shrinkage upon curing, good thermal stability, and excellent thermomechanical properties [17], [18], [19] and [20]. Furthermore, one of the drawbacks of traditional epoxy resins, their brittleness, which severely limits their applications, can be improved by introducing liquid crystalline (LC) domains into the amorphous matrix [21], [22], [23], [24] and [25]. Unlike other toughening methods such as incorporating rubber particles, the presence of LC domains will not lead to a decrease in the glass transition temperature (T_g) or moduli of the material. These desirable properties make LCERs good candidates for a wide range of potential applications, such as optical switches, electronic packaging, and matrices for high performance composites.

Su and coworkers synthesized a main-chain LCER using biphenyl mesogen and studied the effects of chemical structure changes on the thermal and mechanical properties of the resin [26] and [27]. Robinson and coworkers reported a methylstilbene based LCER which exhibited better fracture toughness compared to the same resin cured in amorphous phase [28]. A liquid crystalline phase time–temperature–transformation diagram was also constructed by studying the gelation and vitrification point using oscillatory parallel plate rheology [29] and [30]. Barclay and cowerkers investigated the alignment of a methylstilbene based LCER by applying high strength magnetic field upon curing [31] and [32]. The resulting resin showed a substantial reduction in the coefficient of thermal expansion (CTE) in the direction of orientation compared

to the unaligned samples. While the thermal and mechanical properties of various LCERs have been reported, several fundamental aspects including the nature of LC formation and the thermomechanical properties of fully cured LCERs are still not fully understood.

In this paper, the LC properties and curing behavior of an epoxy resin are examined extensively. The influence of curing condition on the formation of LC phase is investigated. In addition, the LC phase of fully cured resins is characterized using various experimental techniques. The glass transition temperature, dynamic mechanical properties, and thermal expansivity of the resins cured in LC and non-LC state are examined systematically.

2. Experimental section

2.1. Materials

4,4′-dihydroxybiphenyl with 97% purity, benzyltrimethylammonium bromide, and sulfanilamide (SAA) were purchased from Sigma–Aldrich (Milwaukee, WI). Epichlorohydrin with 99% purity was obtained from Acros Organics (Belgium). Sodium hydroxide, isopropyl alcohol, chloroform, methanol, hydrochloric acid, and acetone were supplied by Fisher Scientific (Fair Lawn, NJ). All chemicals were used as received without further purification.

2.2. Synthesis of 4,4′-diglycidyloxybiphenyl (BP)

The epoxy monomer was synthesized according to a procedure reported in an earlier work by Su and coworkers [27]. A mixture of 4,4′-dihydroxybiphenyl (57.26 g), benzyltrimethylammonium bromide (2.09 g) and epichlorohydrin (481 ml) was placed in a three-neck flask and refluxed for 40 min. NaOH (24.6 g) was dissolved in 139 ml of water to prepare 15% NaOH aqueous solution. Then the solution was added into the flask dropwise over a period of 3 h under reflux. The reaction was carried out for an additional hour at room temperature. The excess epichlorohydrin was removed by vacuum distillation and the final product was washed with water and methanol. A white powder was obtained by recrystallization from isopropyl alcohol and chloroform.

2.3. Sample preparation and curing process

Uncured resin samples were prepared by dissolving BP and SAA in tetrahydrofuran (THF) in a stoichiometric ratio. Then the solvent was removed at room temperature and the mixture was dried under vacuum for 24 h to prevent further reaction. To study the curing behavior, the mixture was loaded into aluminum differential scanning calorimeter (DSC) pans and hermetically sealed. A small hole was made in the center of the lids to prevent pressure buildup. To study the thermomechanical properties of fully cured resins, the samples were cured in a convection oven at 170 °C, 180 °C, 190 °C, and 200 °C for 12 h and post-cured at 230 °C for 2 h.

2.4. Characterization of BP and fully cured resins

The chemical structure of BP was characterized using fourier transform infrared spectroscopy (FTIR) and nuclear magnetic resonance (NMR). The FTIR spectrum was recorded on a Bruker's IFS66V FTIR with a resolution of 2 cm^{-1} from 400 to 4000 cm^{-1} at room temperature. The characteristic peaks at 2927 cm^{-1}, 1606 cm^{-1}, 1500 cm^{-1}, 1244 cm^{-1}, 1037 cm^{-1} and 910 cm^{-1} can be assigned to the stretching of (CH_2), stretching of (C═C), bending of (C═C), stretching of (C–O) on aromatic rings, stretching of (C–O) on aliphatic chain, and epoxy group, respectively. The ^1H NMR spectrum was obtained by means of a Varian VXR-300 NMR instrument at room temperature, in the presence of $CDCl_3$ as the solvent. ^1H NMR (CDCl3): δ2.78(2H, dd, CH_2 of epoxy), δ2.93(2H, dd, CH_2 of epoxy), δ3.38(2H, m, CH of epoxy), δ4.01(2H, CH_2 dd, of glycidyl), δ4.25(2H, dd, CH_2 of glycidyl), δ6.96(4H, d, biphenyl), δ7.45(4H, d, biphenyl).

The epoxy equivalent weight (EEW) of BP was determined by titration using the hydrohalogenation method. Concentrated hydrochloric acid was added into dimethylformamide to produce hydrochlorination reagent. Cresol red solution was used as acid-base indicator and was prepared by dissolving cresol red in a mixture of acetone and distilled water. A small amount of BP was dissolved in the hydrochlorination reagent. Then the excess acid was titrated with a 0.1 N sodium hydroxide solution. The EEW was found to be 170.6, which is consistent with the value previously reported by Su [27]. The chemical structures of the epoxy monomer and the curing agent are illustrated in Fig. 1.

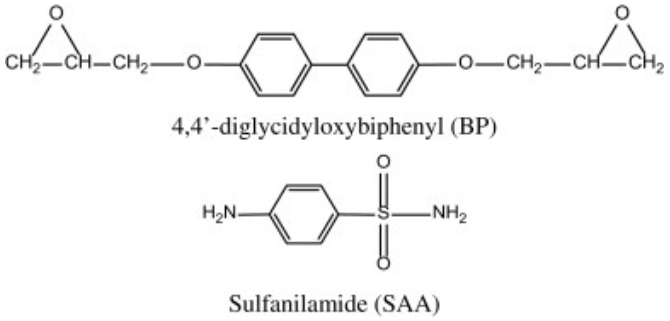

Fig. 1: Chemical structures of the epoxy monomer and the curing agent.

The thermal properties of BP and the fully cured resins were studied using a Q2000 DSC (TA Instruments, Inc.). The DSC cell was purged with helium gas at a flow rate of 25 mL/min. The epoxy monomer was tested at a heating and cooling rate of 10 °C/min. For the fully cured resins, the first heating scan was used to erase the thermal history. While the second heating scan was recorded to evaluate T_g.

To study the curing behavior, the mixture of BP and SAA was loaded into a hermetic aluminum DSC pan then sealed with a lid. A series of isothermal cure studies were carried out using a Q20 DSC (TA Instruments, Inc.). The DSC cell was purged with nitrogen gas at a flow rate of 50 mL/min. The samples were cured at 150 °C, 160 °C, 170 °C, 180 °C, 190 °C, 200 °C, and 210 °C for 180 min respectively.

Morphologies of BP were investigated using a polarized optical microscope (POM) from Olympus (model BX51-TRF equipped with a Linkam LTS-350 hot stage and TMS-94 temperature controller). Small amounts of BP (2∼3 mg) was pre-melted on a microscope slide then covered with a piece of cover glass to form a uniform thin film. The samples were heated and cooled repeatedly from room temperature to 170 °C at a rate of 1 °C/min to investigate the change of birefringence. The isothermal cure of BP with SAA was also monitored using POM. The formation and development of the LC phase were examined under polarized light.

Wide angle X-ray diffraction (WAXD) was used to explore the crystal structure of BP and the fully cured LCERs. For the epoxy monomer, a high temperature XRD experiment was carried out using Rigaku Rint 2000 diffractometer equipped with a high temperature furnace. The diffraction patterns were collected at 30 °C, 100 °C, 140 °C on heating process and 100 °C, 30 °C on cooling process respectively with a Zr-filtered MoKα radiation. In the experiment, a platinum plate was used as a sample holder, and the scan rate was 0.15°/min over a scan angle from 0° to 40°. For the fully cured resins, the diffraction patterns were collected using Scintag XDS2000 powder diffractometer with Kevex Peltier cooled silicon detector and Ni-filtered CuKα radiation. The scan rate was 2°/min over a scan angle from 0° to 40°.

Dynamic mechanical properties of the fully cured resins were studied using a model Q800 dynamic mechanical analyzer (DMA, TA Instruments, Inc.). All the samples were heated from room temperature to 280 °C at 3 °C/min, at 1 Hz frequency and 25 μm amplitude in three-point bending mode.

The coefficient of thermal expansion (CTE) of the fully cured resins was measured with a model Q400 thermomechanical analyzer (TMA, TA Instruments, Inc.) in expansion mode with a heat–cool–heat cycle at a rate of 5 °C/min-3 °C/min-3 °C/min. The second heating scan was recorded to calculate the value of CTE.

Thermal stability of the fully cured LCERs was investigated using thermogravimetric analyzer (TGA) on a model Q50 TGA (TA Instruments, Inc.). About 10 mg of resins was placed in an alumina pan and heated from room temperature to 800 °C at a rate of 20 °C/min under an air purge of 60 mL/min.

3. Results and discussion

3.1. Thermal behavior and morphologies of BP

The DSC thermogram of the epoxy monomer is shown in Fig. 2. Two endothermic peaks were observed in the first heating scan, while in the second heating scan, the first peak was absent. The second peak and the shoulder attached are the melting of BP and its low molecular weight fraction, which was confirmed by Gel permeation chromatography studies.

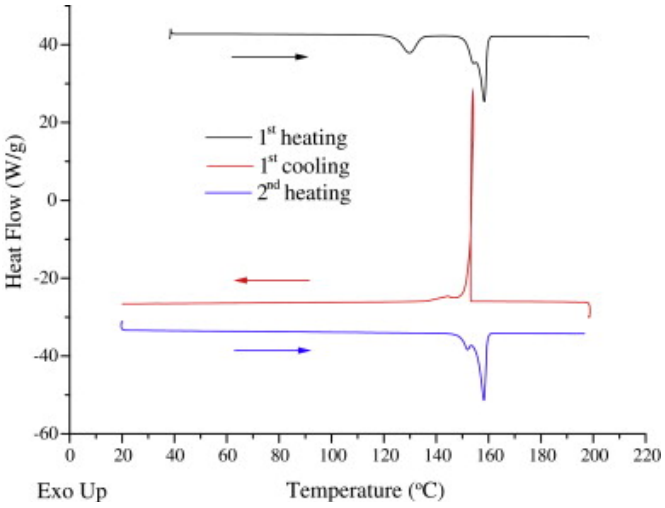

Fig. 2: DSC thermograms of BP.

The monomer was further studied using NMR and high temperature XRD to explore the different thermal behavior in the first and second heating DSC scans. In order to study the effect of the small endothermic peak in the first heating DSC scan on the chemical structure of BP, room temperature NMR spectra of the monomer dried at 100 °C and 140 °C were collected and compared. As shown in Fig. 3, the two NMR spectra have identical peak position and area, indicating that the small endothermic peak in the DSC curve does not have any influence on the chemical structure of the monomer. A change of crystal structure could be a possible explanation for the different thermal behavior observed in the DSC scans.

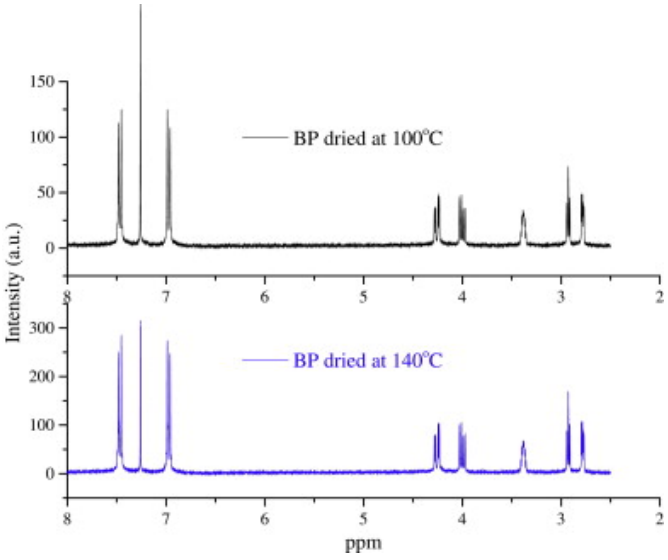

Fig. 3: NMR spectra of BP after drying at 100 °C and 140 °C respectively.

A high temperature XRD experiment was carried to explore the possibility of a structural change. The full diffraction patterns are shown in Fig. 4. The peaks at around 18°, 21°, 29°, 35°, and 36° are the diffraction from platinum sample holder. The shape and position of these peaks remains essentially identical. The slight shift is due to the change of lattice parameter of platinum at different temperatures. However, for the peaks in the region highlighted with dotted line, a distinct change of peak shape and position can be

seen, which indicates that the crystal structure of BP at 100 °C and 140 °C are different. Furthermore, this crystal structure transition is irreversible, which is in agreement with the DSC data. Nevertheless, we were unable to identify the exact crystal structure of BP since it is not a pure compound. Based on the DSC and XRD data, we could conclude that the small endothermic peak in the first heating DSC scan is related to the change of crystal structure of BP and the transition process is irreversible.

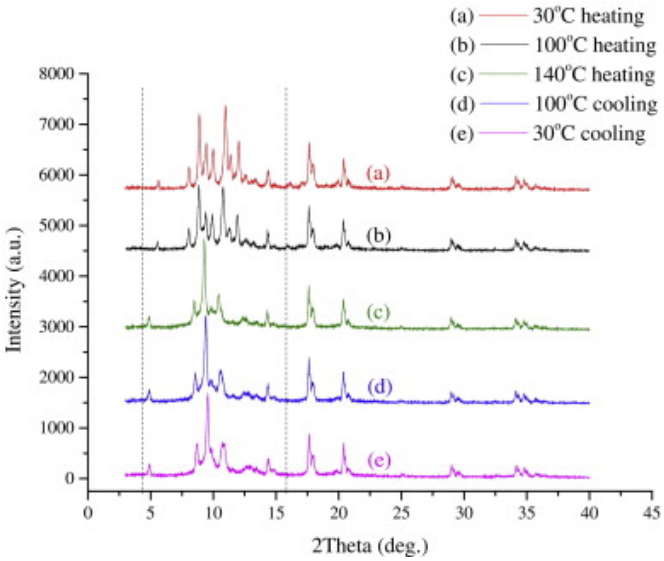

Fig. 4: XRD spectra of BP upon heating and cooling. (a) 30 °C on heating; (b) 100 °C on heating; (c) 140 °C on heating; (d) 100 °C on cooling; (e) 30 °C on cooling.

The thermal behavior of BP is not well understood and there are differing reports in the literature regarding the LC behavior of this monomer. For example, Su and coworkers reported a smectic LC phase in the temperature range of 128–153 °C when the monomer was heated, while Lee and coworkers were not able to detect any LC phase upon heating but observed a smectic LC phase on cooling of the monomer from the isotropic state [27] and [33].

In order to clarify the LC properties of BP, we examined the morphologies at different temperatures under polarized light since it is well known that POM is a powerful tool for characterization of LC phases. POM results shown in Fig. 5 indicate that the monomer starts to melt at 158 °C, in a good agreement with the DSC data. At 164 °C, all the crystallites are melted and the POM image is completely dark. In the cooling process, small crystallites start to grow at about 162 °C and morphologies of the crystallites do not change much after 154 °C. Nematic LC phase usually displays schlieren texture while smectic LC phase usually shows a fan-shaped focal-conic texture. In our studies, no LC birefringence can be observed under polarized light in both heating and cooling processes, indicating that BP is not a LC epoxy monomer.

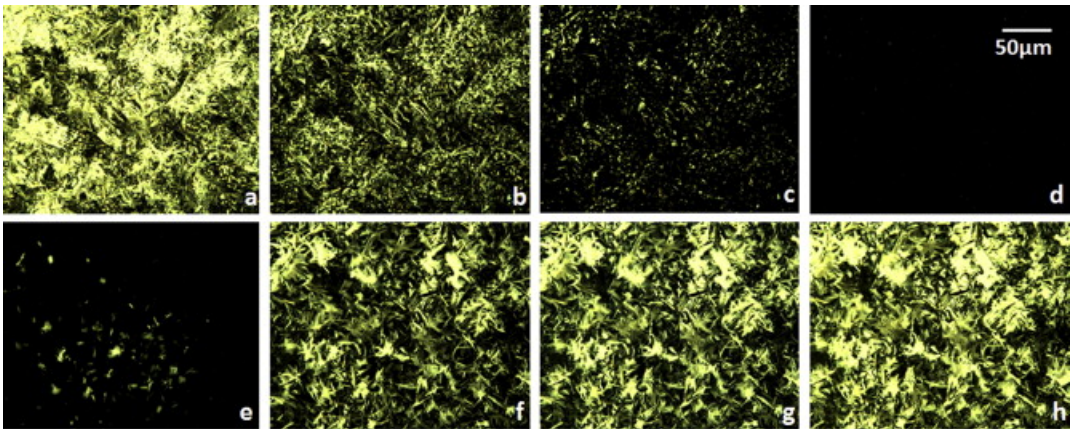

Fig. 5: POM images of BP upon heating and cooling. Heating process: (a) 25 °C, (b) 158 °C, (c) 162 °C, (d) 164 °C. Cooling process: (e) 162 °C, (f) 158 °C, (g) 154 °C, (h) 25 °C.

3.2. Curing behavior and LC properties of the resins

A dynamic DSC scan was performed to study the reaction heat, onset temperature, and peak temperature of the curing reaction, which is important for determining the isothermal curing conditions. As shown in the DSC dynamic scan in Fig. 6, the exothermic curing reaction of BP and SAA starts immediately after the endothermic melting of the two components. The curing reaction has a wide temperature range from 150 °C to 260 °C. When the temperature exceeds 260 °C, the resin starts to decompose, which is indicated by the onset of an exothermic peak shown in the DSC thermogram.

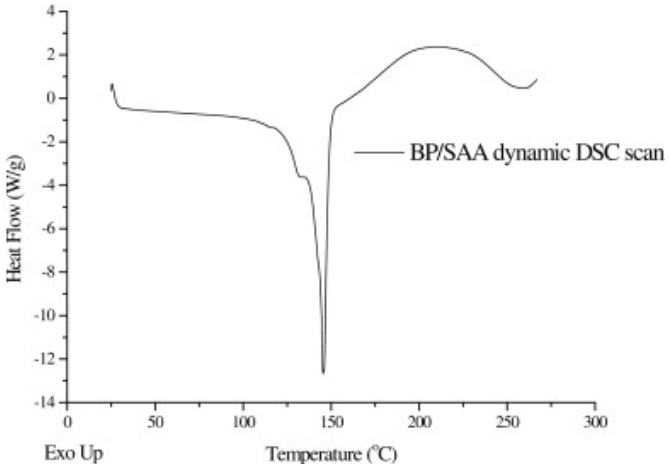

Fig. 6: Dynamic DSC curing study of BP with SAA.

Fig. 7 shows a series of isothermal DSC curing studies of uncured resins. An additional exothermic peak indicated by arrows in the figure was observed for cure temperatures from 150 °C to 190 °C. For cure temperatures of 200 °C and higher, this peak was absent. Similar results have been reported by Carfagna and coworkers for 4,4′-dihydroxy-α-methylstilbene (DOMS) and 2,4-Diaminotoluene (DAT) system [34]. The first exothermic peak represents the reaction between the first epoxy group of the monomer and the

aromatic amine group of the curing agent. SAA is a tetra-functional curing agent and the two amine groups have different reactivity. The aromatic amine tends to react first due to the electron donating effect of the benzene ring, which results in an extension of the pre-polymer chain. If the cure temperatures can be properly chosen, the chain will keep growing without extensive branching. According to Flory's lattice theory of liquid crystalline polymers, when the aspect ratio of the polymer chain is greater than 6.4, the LC phase will be relatively stable and can be detected by POM or other experimental techniques [35]. In our case, for cure temperatures from 150 °C to 190 °C, the curing reaction does not proceed fast; therefore the pre-polymer chain has enough time to extend. After a certain period of time, LC phase becomes more stable with respect to the isotropic phase. At this time, the resins change from transparent to opaque, indicating the existence of the LC phase (Table 1).

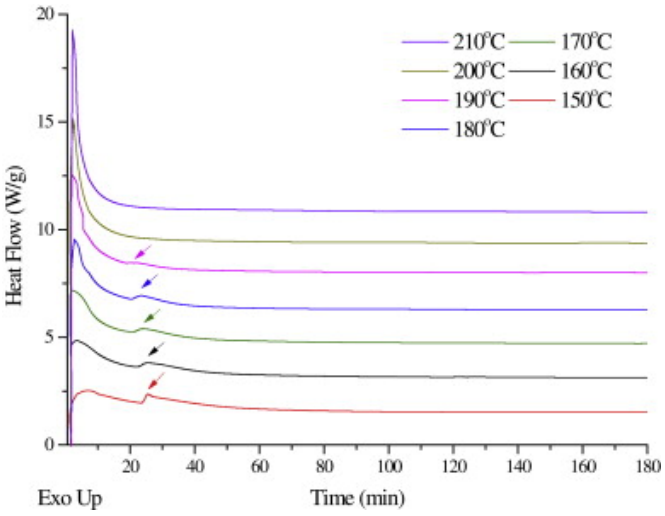

Fig. 7: Isothermal DSC curing study of BP with SAA at different temperatures.

Table 1.
Effect of cure temperatures on the formation of LC phase.

Curing Temperature(°C)	Time second peak appears (min)	Remarks
210 °C	N/A	Non-LC
200 °C	N/A	Non-LC
190 °C	18.26	LC
180 °C	20.29	LC
170 °C	20.80	LC
160 °C	22.17	LC
150 °C	23.37	LC

The second exothermic peak in the isothermal DSC scans is a result of the rate acceleration of the cure reaction when the system undergoes a phase transition from amorphous phase to LC phase. Carfagna and coworkers reported a decrease of viscosity for DOMS/DAT system when

the reacting medium was in the nematic LC phase [34]. Shiota and coworkers studied the smectic structure formation of a liquid crystalline epoxy resin. The rate acceleration was also observed in isothermal DSC measurement and was attributed to a transition when the reacting medium changes from heterogenous to homogenous [36]. In the BP and SAA system examined in this work, the rate acceleration was observed for cure temperatures from 150 °C to 190 °C. At this stage of cure, the residual amine reacts with the epoxy group, leading to the formation of a crosslinked network. The LC phase formed previously is still present in the system so that it can be locked by the crosslinking process. At higher cure temperatures, reaction proceeds fast and the pre-polymer chain does not have time to extend. The crosslinking process happens before the aspect ratio of the polymer chain reaches the above mentioned critical value. The formation of the LC phase will be interrupted and the resins will be cured in the amorphous phase. This could explain the absence of the additional exothermic peak for cure temperatures higher than 200 °C

The curing behavior and the LC properties of the resins were also studied using POM. Based on the DSC data, the isothermal temperature was fixed at 170 °C and the whole curing process was recorded in the microscope to examine the formation of the LC phase. Fig. 8 shows several POM images taken at different reaction times. All the pictures were taken from the same area of the same sample. The LC birefringence starts to appear after 19 min of the cure reaction, which is close to the time when the second exothermic peak starts to form in the DSC scan. The isothermal curing studies were also carried out for cure temperatures at 180 °C, 190 °C, and 200 °C under POM. The sample was continuously heated at different temperatures for 2 h to complete the cure reaction, and then morphologies of the fully cured resins were analyzed. The POM images are shown in Fig. 9. The fan-shaped focal-conic texture for the cure temperatures from 170 °C to 190 °C in the figure is a characteristic of the smectic LC phase. The results prove that the LC phase formed in the early stage of the cure reaction has been successfully retained by the crosslinking networks. The results also show that as the cure temperature increases, the smectic LC phase gradually loses its fan-shaped focal-conic texture. For the cure temperature of 200 °C, the POM image is completely dark, indicating the amorphous structure of the resin. The POM study also revealed that the resins cured in LC phase exhibit a polydomain structure with individual LC domain distributed in an amorphous resin matrix.

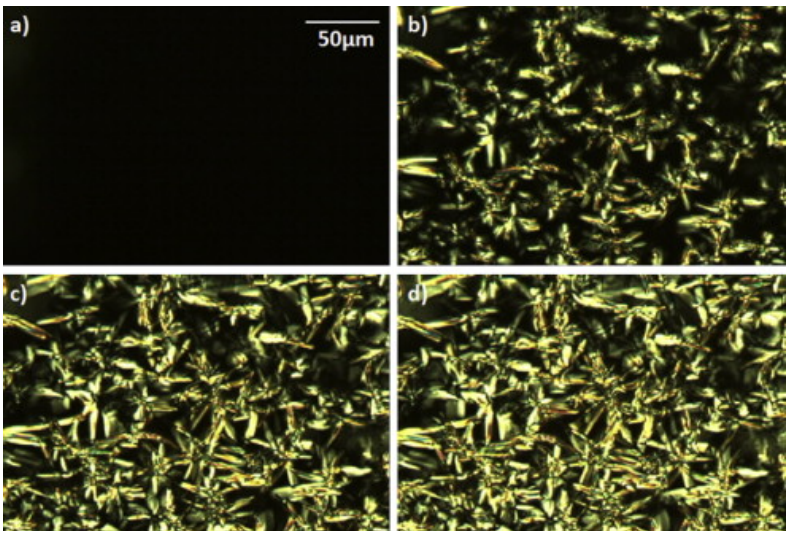

Fig. 8: POM images of isothermal curing study of BP with SAA at 170 °C. (a) 18 min; (b) 20 min; (c) 22 min; (d) 24 min.

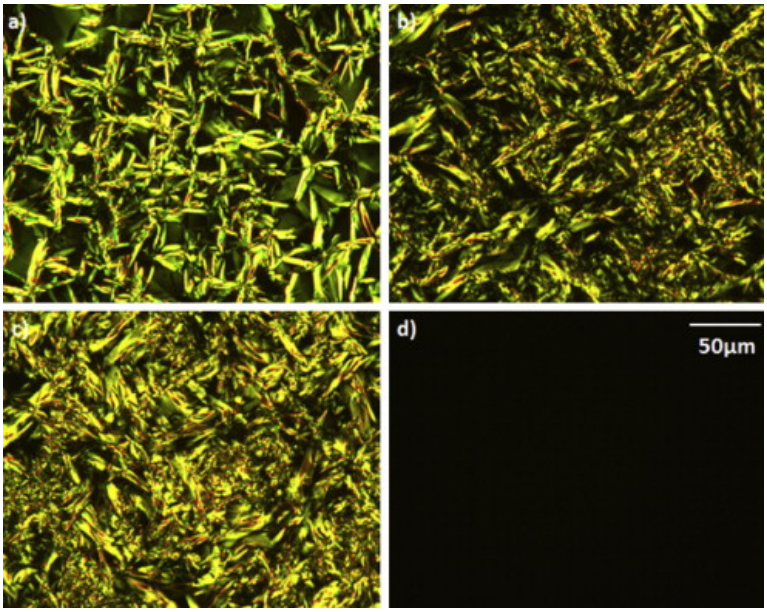

Fig. 9: POM images after 2 h of isothermal cure of BP with SAA at different temperatures. (a) 170 °C; (b) 180 °C; (c) 190 °C; (d) 200 °C.

3.3. Thermal and mechanical properties of LCERs

Bulk samples were cured in a convection oven at 170 °C, 180 °C, and 190 °C for 12 h to produce LCERs with different LC content. Non-LCERs were also prepared by curing the resin at 200 °C for 12 h. After the initial cure, all the samples were post-cured at 230 °C for 2 h to complete the cure reaction as well as to relax any internal residual stress. A visual comparison between the resins cured at different temperatures is provided in Fig. 10.

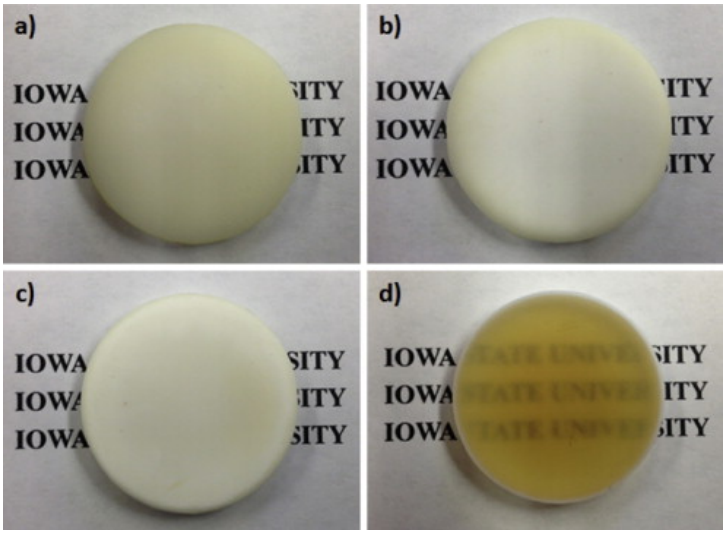

Fig. 10: Photos of the resins cured at different temperatures showing different optical properties. (a) 170 °C; (b) 180 °C; (c) 190 °C; (d) 200 °C.

The resins with LC domains are opaque due to the light scattering at the boundaries of the liquid crystalline and amorphous regions whereas non-LCERs, which were completely amorphous, are transparent, as shown in the same figure. XRD was also used to confirm the existence of LC phases. The XRD spectra of the LCERs and non-LCERs are compared in Fig. 11. A small peak at 4.365° having d-spacing of 20.225 Å was observed for LCERs while this peak is absent in the case of non-LCERs. The smectic LC phase is characterized by its layered structure. The d-spacing calculated from the XRD spectra indicates that the LCERs have layer spacing about 20 Å and have a smectic LC structure. The chemical structure of the mesogen in LCERs was simulated using ChemBio3D software as shown in Fig. 12. The mesogenic length was found to be 20.4 Å which was measured by calculating the bond length after minimizing the energies of the molecules. The distance between two sulfur atoms was used as the mesogenic length. Good agreement between the experimental data and the simulation was obtained, adding further evidence to the presence of a smectic phase in the LCERs.

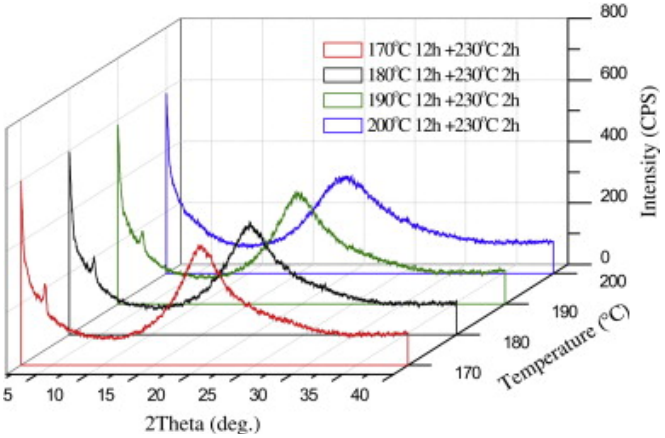

Fig. 11: XRD spectrum of the resins at different temperatures.

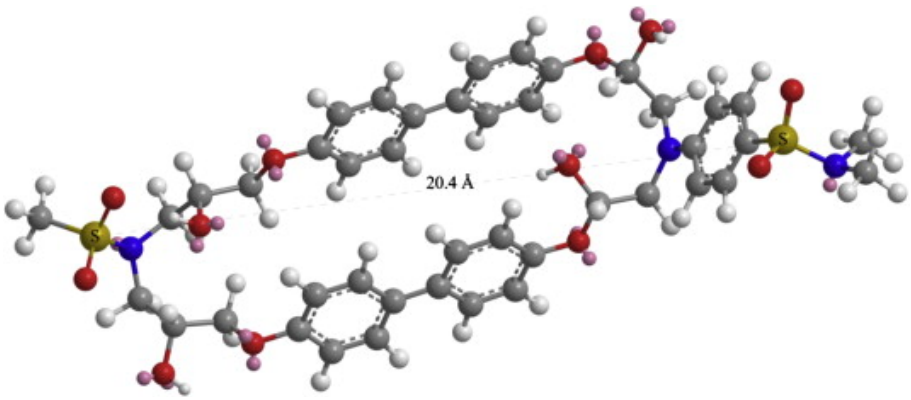

Fig. 12: Chemical structure simulation of the mesogen and network of the LCERs.

The dynamic mechanical properties, as well as the glass transition temperature of the resins were investigated using dynamic mechanical analysis (DMA). The storage modulus (E′) and loss modulus (E″) were determined from the in-phase and out-of-phase response of the resins to an applied strain,

representing the elastic and viscous portions respectively. Moreover, the T_g was measured from the peak of the mechanical damping curve (tan δ) which was the ratio of E″ to E′. The DMA curves of the resins cured at different temperatures are shown in Fig. 13 and the DMA data is summarized in Table 2. For semicrystalline polymers, crystallites have a great influence on the elastic modulus of the materials. As shown in Table 2, LCERs have higher storage moduli in the glassy region (35 °C) compared to non-LCERs, which is due to the presence of LC domains. The rigid and ordered structure of the LC domains has higher moduli compared to the amorphous parts, so they behave as rigid fillers in the resin matrix.

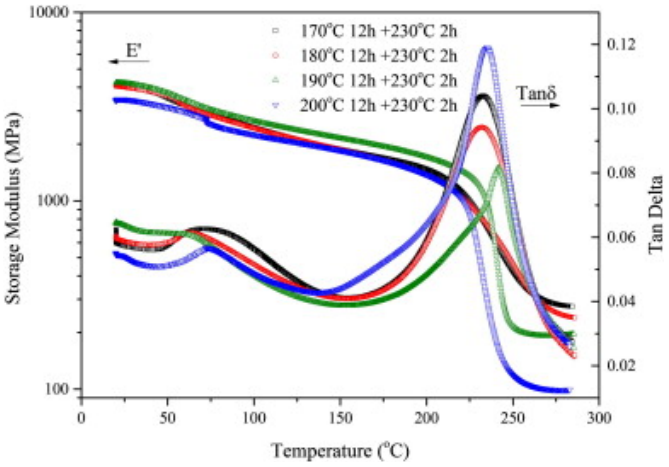

Fig. 13: Temperature dependence of dynamic mechanical properties of the resins cured at different temperatures.

Table 2.
Thermomechanical data obtained from DMA, DSC and TMA.

Cure schedule	E′ at 35 °C (MPa)	E′ at 270 °C (MPa)	T_g [a] (°C)	T_g [b] (°C)	T_g [c] (°C)	CTE[d] (°C)	T_d [e] (°C)	Remarks
170 °C 12 h plus 230 °C 2 h	3975 ± 55	270 ± 8	232.6	206.2	190.8	63.7	306.3	LCER
180 °C 12 h plus 230 °C 2 h	3940 ± 14	244 ± 2	231.5	205.2	191.4	69.6	307.0	LCER
190 °C 12 h plus 230 °C 2 h	4159 ± 34	196 ± 2	241.2	209.2	191.6	64.9	307.7	LCER
200 °C 12 h plus 230 °C 2 h	3422 ± 20	99 ± 0.3	233.3	196.9	183.3	61.1	309.5	Non-LCER

a Taken from the peak of tan δ (DMA).

b Taken from the intercept of the slopes of glassy region and rubber region (TMA).

c Taken from dynamic scans at 20 °C/min (DSC).

d Measured in the temperature range from 50 °C to 70 °C via TMA.

e At 5% weight loss (TGA).

LCERs also show higher storage moduli in the rubbery plateau region, which can be attributed to two reasons. First, in addition to the filler effect mentioned earlier, the LC domains also act as crosslinks, tying segments of the polymer chain together [37]. They do not relax or become soft at temperatures higher than T_g, and therefore the movements of the polymer chains are restricted by these rigid LC domains. Second, the higher rubbery moduli of LCERs could be a result of the reduced viscosity and the accelerated reaction rate when the curing process proceeds in the LC phase, as mentioned previously, which leads to a higher crosslink density for LCERs.

The T_g measured from the peak of the tan δ curve also shows that LCERs have higher T_g compared to non-LCERs. Both of the rigid filler effect and the crosslink effect are responsible for the high T_g observed in LCERs. The free volume of the LCERs is significantly reduced due to the presence of LC domains, thereby decreasing the mobility of the segments in response to an applied thermal energy. The T_g of the resins was also measured using DSC and TMA which is in agreement with the DMA results. In DSC, the T_g is characterized by a step change in the heat capacity of the material, while in TMA the T_g is determined in terms of the change in CTE when the material undergoes a change from glass to rubber. Although measured through three different

experimental techniques, LCERs always show higher T_g than non-LCERs. It is noted that the absolute values of T_g measured in each technique is different, which is not unexpected since the underlying property being monitored is not the same. For example, the T_g measurement in DSC involves monitoring a thermodynamic property (heat capacity) whereas the T_g in DMA is obtained from a viscoelastic property (tan δ).

Thermal expansivity of the LCERs and non-LCERs were evaluated using thermomechanical analysis. Results are summarized in Table 2. Since thermal history has a great effect on the thermomechnical properties of polymers, all the samples were heated to 250 °C to erase the thermal history and release any internal residual stress. Second heating scans were recoded to examine the CTE of the resins. As shown in Table 2, the CTE of the resins cured in LC and non-LC state are quite close, which can be attributed to the random distribution of the LC domains in the amorphous matrix.

Thermal stability of the LCERs and non-LCERs was also investigated. Fig. 14 shows the TGA curves for all the samples. The thermal decomposition temperature (T_d) was defined as the temperature when the samples lost 5% of its initial weight, and the results are summarized in Table 2. TGA data shows that the presence of LC domains does not have a significant influence on the thermal stability of the resins, which indicates that the most important factor that affects the thermal decomposition of a polymeric material is the chemical bonding rather than morphology. In this work, the dynamic mechanical properties and T_g were significantly better for epoxy resins comprising an LC phase. Prior work in the literature has shown that alignment of LC domains may be possible by applying an external field [32], [38], [39] and [40]. The effect of aligning the LC phase in BP/SAA systems using an external electrical or magnetic field and the effect on ensuing anisotropic thermomechanical and dynamic mechanical properties will be examined in future work.

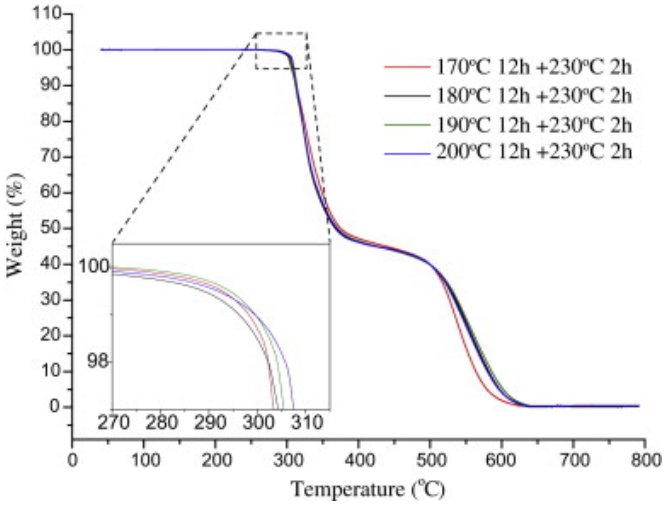

Fig. 14: Thermogravimetric analysis of resins cured at different temperatures.

4. Conclusions

The epoxy monomer BP was successfully synthesized and characterized using various experimental techniques. Results show that BP is not a liquid crystalline epoxy monomer itself and an irreversible crystal transition exists in the temperature range of 120 °C–140 °C. However, upon reacting with SAA, a smectic LC phase starts forming after 20 min of the curing reaction. Cure temperature has a great influence on the formation and development of LC phase and an isotropic network is obtained for cure temperatures greater than 200 °C. A rate acceleration of the curing reaction was observed for the resins cured in the LC phase. The effects of the presence of LC phase on the thermal and mechanical properties of the resins were also investigated. LCERs showed higher values of storage modulus in both glassy region and rubbery plateau region compared to non-LCERs, which is due to the rigid structure of the LC domains and reduced viscosity of the system. The glass transition temperature of the resins cured in LC and non-LC state was studied using DMA, DSC, and TMA respectively. All the results show that LCERs have higher T_g because of the rigid filler and crosslink effects of the LC domains, which results in lower mobility of the polymer chain. The presence of LC phase does not have a significant influence on the coefficient of thermal expansion and thermal stability of the resins, possibly due to the random distribution and orientation of the LC domains.

Acknowledgments

Support under Air Force Office of Scientific Research (AFOSR) Award No. FA9550-12-1-0108 is gratefully acknowledged.

References

[1] G.G. Barclay, C.K. Ober. Progress in Polymer Science, 18 (5) (1993), pp. 899–945.

[2] A. Shiota, C.K. Ober. Progress in Polymer Science, 22 (5) (1997), pp. 975–1000.

[3] E.P. Douglas. Liquid crystalline thermosets. Encyclopedia of polymer science and technology, John Wiley & Sons, Inc. (2002) .

[4] C. Carfagna, E. Amendola, M. Giamberini. Macromolecular Chemistry and Physics, 195 (7) (1994), pp. 2307–2315.

[5] E. Amendola, C. Carfagna, M. Giamberini, G. Pisaniello. Macromolecular Chemistry and Physics, 196 (5) (1995), pp. 1577–1591.

[6] W. Mormann, M. Brocher. Macromolecular Chemistry and Physics, 197 (6) (1996), pp. 1841–1851.

[7] W. Mormann, M. Broche, P. Schwarz. Macromolecular Chemistry and Physics, 198 (11) (1997), pp. 3615–3626.

[8] Q.H. Lin, A.F. Yee, H.J. Sue, J.D. Earls, R.E. Hefner. Journal of Polymer Science Part B-Polymer Physics, 35 (14) (1997), pp. 2363–2378.

[9] D. Rosu, A. Mititelu, C.N. Cascaval. Polymer Testing, 23 (2) (2004), pp. 209–215.

[10] R.A.M. Hikmet, J. Lub, P.M. Vanderbrink. Macromolecules, 25 (16) (1992), pp. 4194–4199.

[11] M.H. Litt, W.-T. Whang, K.-T. Yen, X.-J. Qian. Journal of Polymer Science Part A: Polymer Chemistry, 31 (1) (1993), pp. 183–191.

[12] D. Holter, H. Frey, R. Mulhaupt, J.E. Klee. Macromolecules, 29 (22) (1996), pp. 7003–7011.

[13] A.E. Hoyt, B.C. Benicewicz. Journal of Polymer Science Part A-Polymer Chemistry, 28 (12) (1990), pp. 3403–3415.

[14] A.E. Hoyt, B.C. Benicewicz. Journal of Polymer Science Part A-Polymer Chemistry, 28 (12) (1990), pp. 3417–3427.

[15] G.G. Barclay, C.K. Ober, K.I. Papathomas, D.W. Wang. Macromolecules, 25 (11) (1992), pp. 2947–2954.

[16] W. Mormann, J. Zimmermann. Liquid Crystals, 19 (2) (1995), pp. 227–233.

[17] C. Carfagna, E. Amendola, M. Giamberini. Composite Structures, 27 (1–2) (1994), pp. 37–43.

[18] C. Carfagna, E. Amendola, M. Giamberini. Progress in Polymer Science, 22 (8) (1997), pp. 1607–1647.

[19] P. Kannan, P. Sudhakara. Liquid crystalline thermoset epoxy resins. High performance polymers and engineering plastics, John Wiley & Sons, Inc. (2011), pp. 387–422.

[20] M. Giamberini, E. Amendola, C. Carfagna. Molecular crystals and liquid crystals science and technology section A-molecular crystals and liquid crystals, 266 (1995), pp. 9–22.

[21] H.J. Sue, J.D. Earls, R.E. Hefner. Journal of Materials Science, 32 (15) (1997), pp. 4031–4037.

[22] C. Ortiz, R. Kim, E. Rodighiero, C.K. Ober, E.J. Kramer. Macromolecules, 31 (13) (1998), pp. 4074–4088.

[23] C. Ortiz, L. Belenky, C.K. Ober, E.J. Kramer. Journal of Materials Science, 35 (8) (2000), pp. 2079–2086.

[24] M. Harada, K. Aoyama, M. Ochi. Journal of Polymer Science Part B-Polymer Physics, 42 (22) (2004), pp. 4044–4052.

[25] M. Harada, N. Okamoto, M. Ochi. Journal of Polymer Science Part B-Polymer Physics, 48 (22) (2010), pp. 2337–2345.

[26] W.F.A. Su. Journal of Polymer Science Part A-Polymer Chemistry, 31 (13) (1993), pp. 3251–3256.

[27] W.F.A. Su, K.C. Chen, S.Y. Tseng. Journal of Applied Polymer Science, 78 (2) (2000), pp. 446–451.

[28] E.J. Robinson, E.P. Douglas, J.J. Mecholsky. Polymer Engineering and Science, 42 (2) (2002), pp. 269–279.

[29] S.H. Cho, E.P. Douglas. Macromolecules, 35 (11) (2002), pp. 4550–4552.

[30] S. Cho, E.P. Douglas, J.Y. Lee. Polymer Engineering and Science, 46 (5) (2006), pp. 623–629.

[31] G.G. Barclay, C.K. Ober, K.I. Papathomas, D.W. Wang. Journal of Polymer Science Part A-Polymer Chemistry, 30 (9) (1992), pp. 1831–1843.

[32] G.G. Barclay, S.G. McNamee, C.K. Ober, K.I. Papathomas, D.W. Wang. Journal of Polymer Science Part A-Polymer Chemistry, 30 (9) (1992), pp. 1845–1853.

[33] J.Y. Lee, J.S. Jang, S.S. Hwang, S.M. Hong, K.U. Kim. Polymer, 39 (24) (1998), pp. 6121–6126.

[34] C. Carfagna, E. Amendola, M. Giamberini, A.G. Filippov, R.S. Bauer. Liquid Crystals, 13 (4) (1993), pp. 571–584.

[35] P.J. Flory, G. Ronca. Molecular Crystals and Liquid Crystals, 54 (3–4) (1979), pp. 311–330.

[36] A. Shiota, C.K. Ober. Polymer, 38 (23) (1997), pp. 5857–5867.

[37] L.E. Nielsen, F.D. Stockton. Journal of Polymer Science Part A: General Papers, 1 (6) (1963), pp. 1995–2002.

[38] B.C. Benicewicz, M.E. Smith, J.D. Earls, R.D. Priester, S.M. Setz, R.S. Duran, *et al.* Macromolecules, 31 (15) (1998), pp. 4730–4738.

[39] S. Jahromi, W.A.G. Kuipers, B. Norder, W.J. Mijs. Macromolecules, 28 (7) (1995), pp. 2201–2211.

[40] C.B. Tan, H. Sun, B.M. Fung, B.P. Grady. Macromolecules, 33 (17) (2000), pp. 6249–6254.